Supporting Information

Polymeric perfluorocarbon nanoemulsions are ultrasound-activated wireless drug infusion catheters

Zhong, Q[†1,2], Yoon BC[†1,3], Aryal M[1], Wang JB[1], Ilovitsh T[1,4], Baikoghli MA[5], Hosseini-Nassab N[1], Karthik A[1], Cheng RH[5], Ferrara KW[1,4], Airan RD[1]*

1. Department of Radiology, Stanford University, Stanford, CA 94305, U.S.A.

2. David H. Koch Institute for Integrative Cancer Research, Massachusetts Institute of Technology, Cambridge, MA 02139

3. Department of Radiology, Massachusetts General Hospital, Boston, MA 02114

4. Department of Biomedical Engineering, University of California, Davis, CA 95616, U.S.A.

5. Department of Molecular and Cellular Biology, University of California, Davis, CA 95616, U.S.A

† These authors contributed equally to this work.

* To whom correspondence should be addressed:
Raag Airan MD PhD
Departments of Radiology (Neuroradiology) and, by courtesy, Materials Science & Engineering
Stanford University
300 Pasteur Drive, Grant Rm. S043
Stanford, CA 94305
Office: 650-724-1190
Fax: 650-736-6767

Supplementary Methods

S1. Removal of Hydrochloride from Drug Molecules

The base form of ketamine, doxorubicin, nicardipine, and verapamil was prepared by removing hydrochloride from the purchased chemicals for further encapsulation in the nanoemulsions. The drug molecule was dissolved in a solvent (doxorubicin hydrochloride: 2 mg/ml in DI water; ketamine hydrochloride: 2 mg/ml in saline; nicardipine hydrochloride: 2 mg/ml in 2:1 DI water:methanol (v:v); verapamil hydrochloride: 2 mg/ml in DI water). 3 N NaOH was added to neutralize the hydrochloride. A two-fold volume of chloroform was used to extract the drug base molecule from the aqueous phase three times. The combined chloroform phase was dried over anhydrous sodium sulfate. After complete evaporation of chloroform, the drug was sealed in a glass vial and stored at -20 °C for future use.

S2. Dynamic Light Scattering (DLS)

A 10 µl nanoemulsion solution was thoroughly mixed with 990 µl cold PBS. DLS parameters were: materials = perfluoropentane; refractive index (RI) = 1.330; absorption = 0.1; dispersant = ICN PBS tablets; viscosity = 0.8882 cP at 25 °C; Mark-Houwink parameters; equilibration time = 60 s; disposable cuvettes = ZEN0118; measurement angle = 90 degree; measurement duration = automatic; number of measurements = 5; positioning method = seek optimum position; analysis model = general purpose (normal resolution). To measure the zeta potential, 10 µl nanoemulsion solution was mixed with 990 µl deionized water. Then 990 µl of this solution was transferred to a disposable capillary cell. Measurement parameters were: cell type = DTS1070, dispersant = water; viscosity = 0.8872 cP at 25 °C; dielectric constant = 78.54; F(κa) selection model = Smoluchowski; F(κa) value =1.5; measurement duration = automatic; measurement runs between 10 and 100; number of measures = 3 with no delay between measurements.

S3. Quantification of Drug Loading in Nanoemulsions

a. **Propofol and doxorubicin**. A 100 µl nanoemulsion solution was thoroughly mixed with 900 µl methanol. The fluorescence of drug was quantified with a Tecan Infinite M1000 microtiter plate reader (Tecan Instruments. San Jose, CA, USA) for propofol at the excitation/emission = 276/302 nm and doxorubicin at 500/595 nm, respectively. The drug content was calculated with respect to a standard curve of the drug prepared in varying concentrations in the same solvent.

b. **Ketamine, nicardipine, verapamil and dexmedetomidine**. A 100 µl nanoemulsion solution was thoroughly mixed with 900 µl methanol. The UV absorbance was measured with a Varian Cary 50 UV-VIS spectrophotometer (Agilent Technologies; Santa Clara, CA, USA) for ketamine at 280 nm, nicardipine at 348 nm, verapamil at 282 nm and dexmedetomidine at 262 nm, respectively. The drug

content was calculated with respect to a standard curve of the drug prepared in varying concentrations in the same solvent.

c. **Cisplatin**. The amount of cisplatin encapsulated in the nanoemulsion was measured according to a previously reported method with minor modifications [1]. A 100 µl nanoemulsion suspension was added to 1.9 ml pH 6.8 PBS (10 mM) and then mixed up with 1 ml ortho-phenylenediamine (OPDA) DMF solution (1.4 mg/ml). The mixture was heated at 105 °C for 20 min. The solution was cooled down to room temperature and the UV absorbance at 703 nm was immediately measured with a Varian Cary 50 UV-VIS spectrophotometer. The content of cisplatin was calculated with respect to a standard curve of the drug prepared in varying concentrations in the same solvent.

S4. Cryo-Electron Microscopy

Cyro-electron microscopy (EM) was performed on a JEM 2100F cryo-TEM (JEOL, Peabody MA) operating at 200kV, using previously described protocols [2,3]. Briefly, a volume of 3.5 µl sample solution containing the nanodroplets of a final concentration ~1.5 µg/ml was placed on Quantifoil R2/2 Cu 300 mesh grids. After an incubation of 1.5 minutes, 0.5 µl of NP40 detergent was added for another 15 seconds before the subsequent blotting. The excess solution was removed by manual blotting and quickly plunged into liquid ethane. The frozen-hydrated grids were transferred into the EM using a Gatan 626 cryo-transferring system. The specimen was examined at 40,000x magnification and images were captured using a direct electron detector (DE-20, San Diego CA) with a pixel size of 1.3 Angstroms using SerialEM (University of Colorado, Boulder) autofocusing control option with defocus range set to 1.5-4.5 microns. Digital frames were motion corrected with MotionCorr2 (University of California, San Francisco) software and with no stigmatism or drift detected prior to further image processing, analysis, and figure preparation.

S5. Chromogenic Limulus Amebocyte Lysate (LAL) Endotoxin Assay

LAL, chromogenic substrate, color-stabilizer #1, #2 and #3, and 1 EU/mL standard endotoxin solution were reconstituted in the provided water or buffers according to the product protocol (Protocol#: L00350). Two sets of standard solutions with varied endotoxin concentrations were prepared to generate standard curves for two different ranges of endotoxin concentration (i.e. 0.01-0.1 EU/ml and 0.1-1.0 EU/ml) due to unknown endotoxin level. A 100 µl sample of reconstituted LAL solution was added to each vial with a 100 µl endotoxin standard solution or nanoparticle solution. All samples were incubated in a 37±1 °C water bath 30 min for the set of 0.01-0.1 EU/ml or 9 min for the set of 0.1-1.0 EU/ml. A 100 µl stop buffer with color-stabilizer #1 was added to each vial, followed by 6 min incubation at 37 ± 1 °C. The 0.5 ml color-stabilizer #2 and #3 were then added, respectively. The UV absorbance of each sample was measured at

545 nm and endotoxin concentration was calculated according to the standard curve acquired in the meantime. ⩽5 EU per 1 mg propofol was considered acceptable endotoxin concentration.

S6. Detection of Bacterial Contamination by Agar Plate Test

The LB agar plate was prepared by adding 30.5 g LB agar powder to 1 L Millipore water and heating to boiling while stirring. The media was autoclaved 15 min at 121°C for sterilization. The media was cooled down slightly, and 10-15 ml was poured into a sterile petri dish. The agar plate was allowed to solidify. The plates can be used fresh or stored at 4°C for future use.

LB media was reconstituted from 15.5 g LB powder with 1 L Millipore water and was autoclaved at 121 °C for 15 min for sterilization. The sterile media was stored at 4 °C for further use. *E. coli* competent cells were cultured in LB media at 37 °C and 200 rpm for 24 h, which was then used as positive control of bacteria. A 50 μL sample (sterile PBS, propofol-loaded PFP nanoemulsion, or positive control) was added to the center of LB agar plate and then distributed evenly with a sterile bacterial spreader. When the liquid was absorbed, the petri dish was recapped, and then turned upside down to prevent condensation during incubation. The plate was incubated for 72 h at 37 °C. The dish was then removed from the incubator and examined for the appearance of colonies.

Supplementary Figures

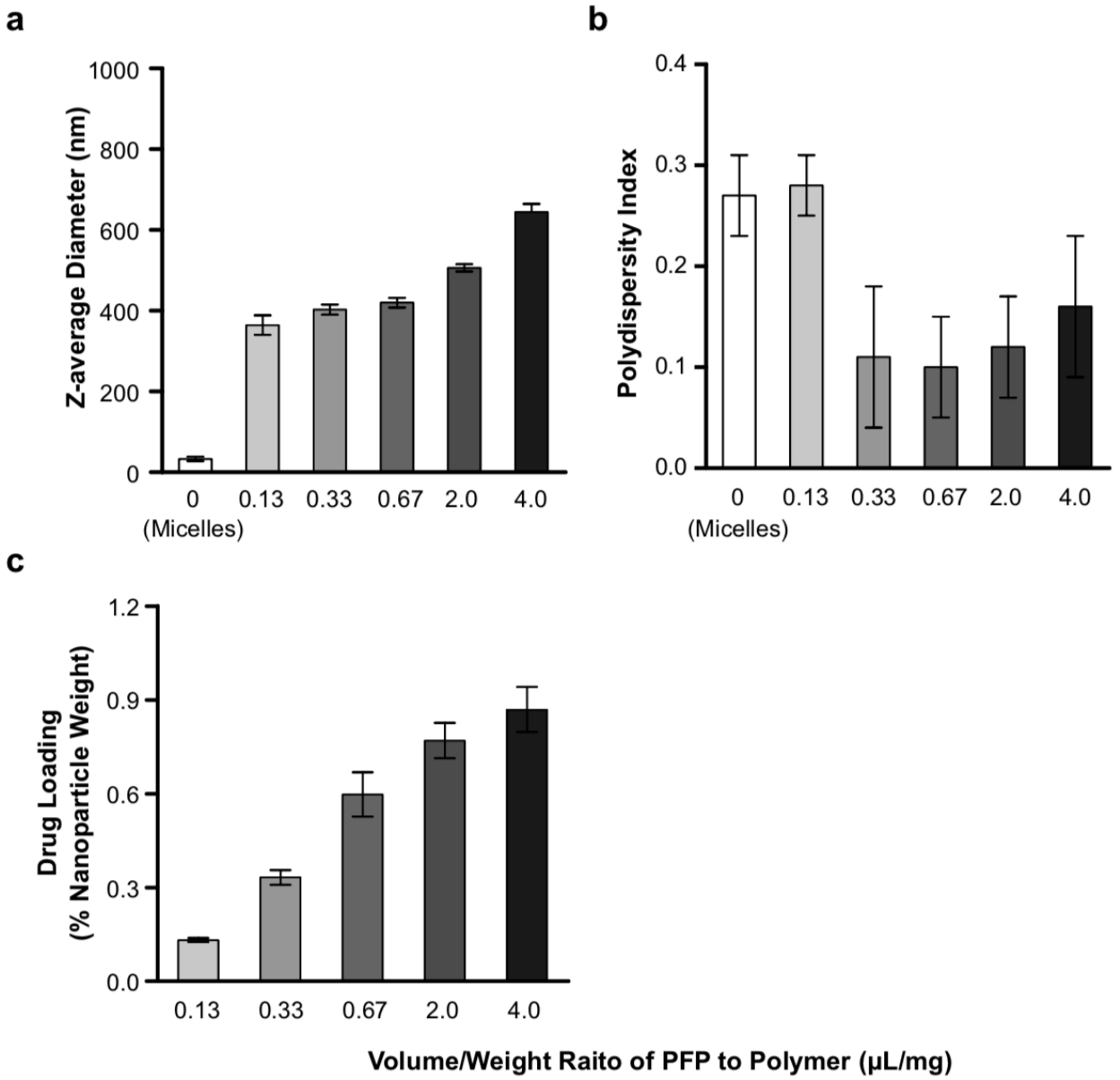

Fig. S1. Effect of perfluoropentane (PFP) volume on physicochemical properties of propofol-loaded nanoemulsions. (a) Z-average diameter, **(b)** polydispersity index and **(c)** drug loading of propofol-loaded nanoemulsions with different volume/weight ratio of PFP to di-block copolymer. 0 μL/mg represents the polymeric micelle suspension.

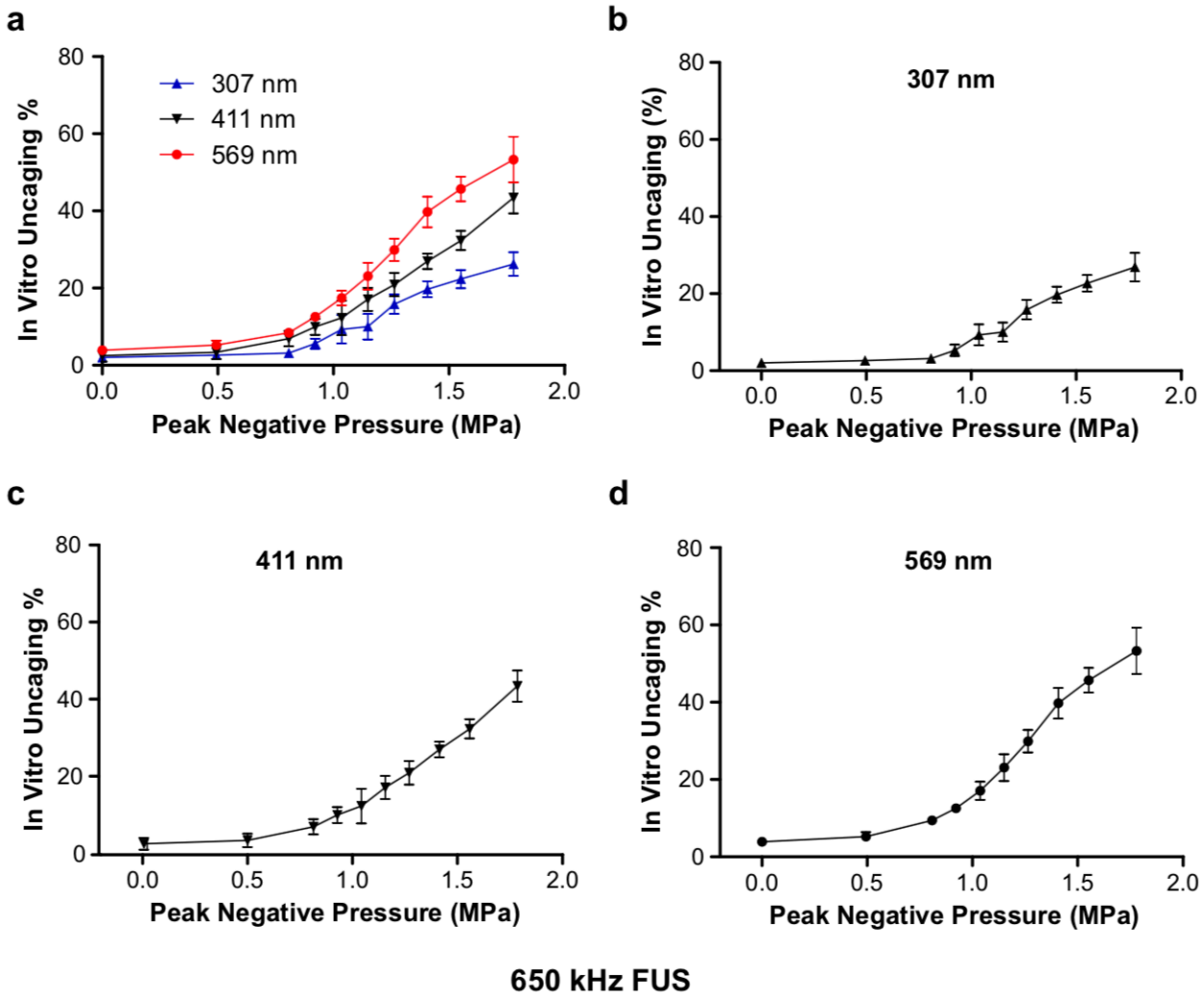

Fig. S2. Effect of particle size on *in vitro* uncaging efficacy of propofol-loaded nanoemulsions. Uncaging efficacy as the percent uncaging of the initial loaded drug for particles of the indicated size, presented on a single plot **(a)**, or individual plots **(b-d)**.

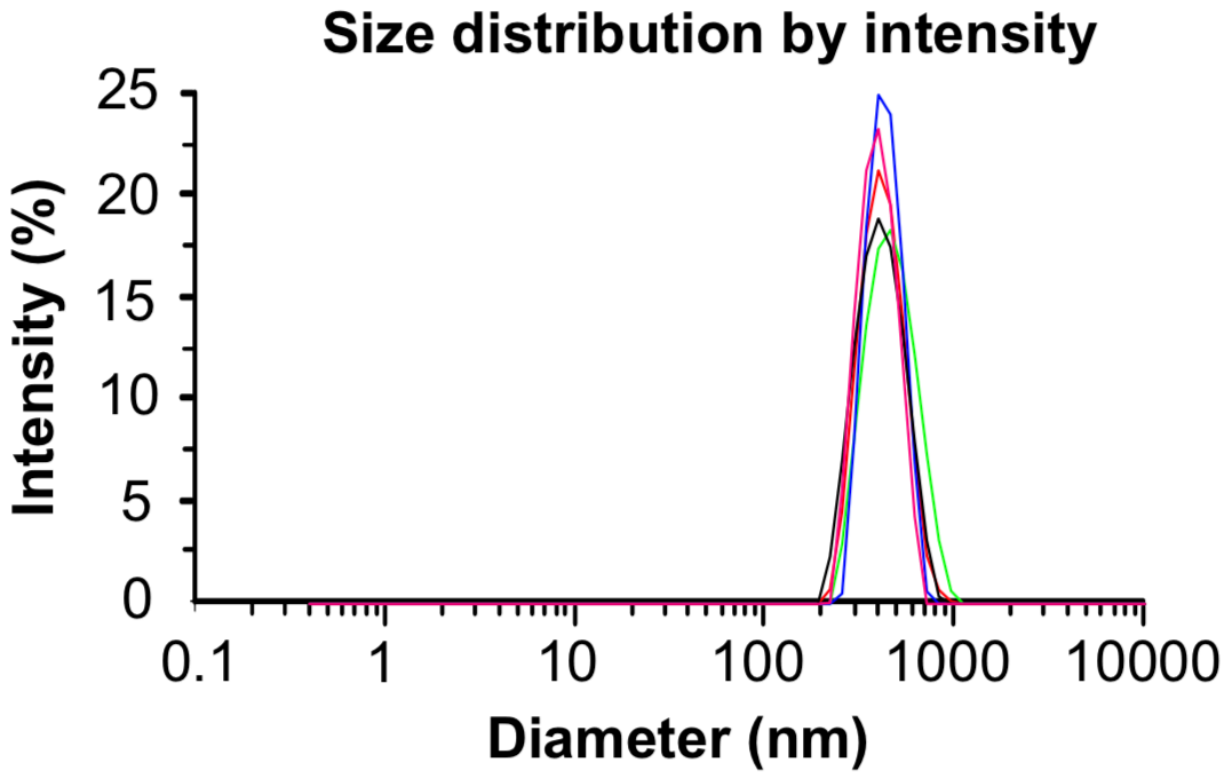

Figure S3. Typical example of DLS spectrum of perfluoropentane polymeric nanoemulsions. For these samples, Z-average diameter was 405.3 ± 22.7 nm, polydispersity index was 0.061 ± 0.033, mean ± S.D. for N=3.

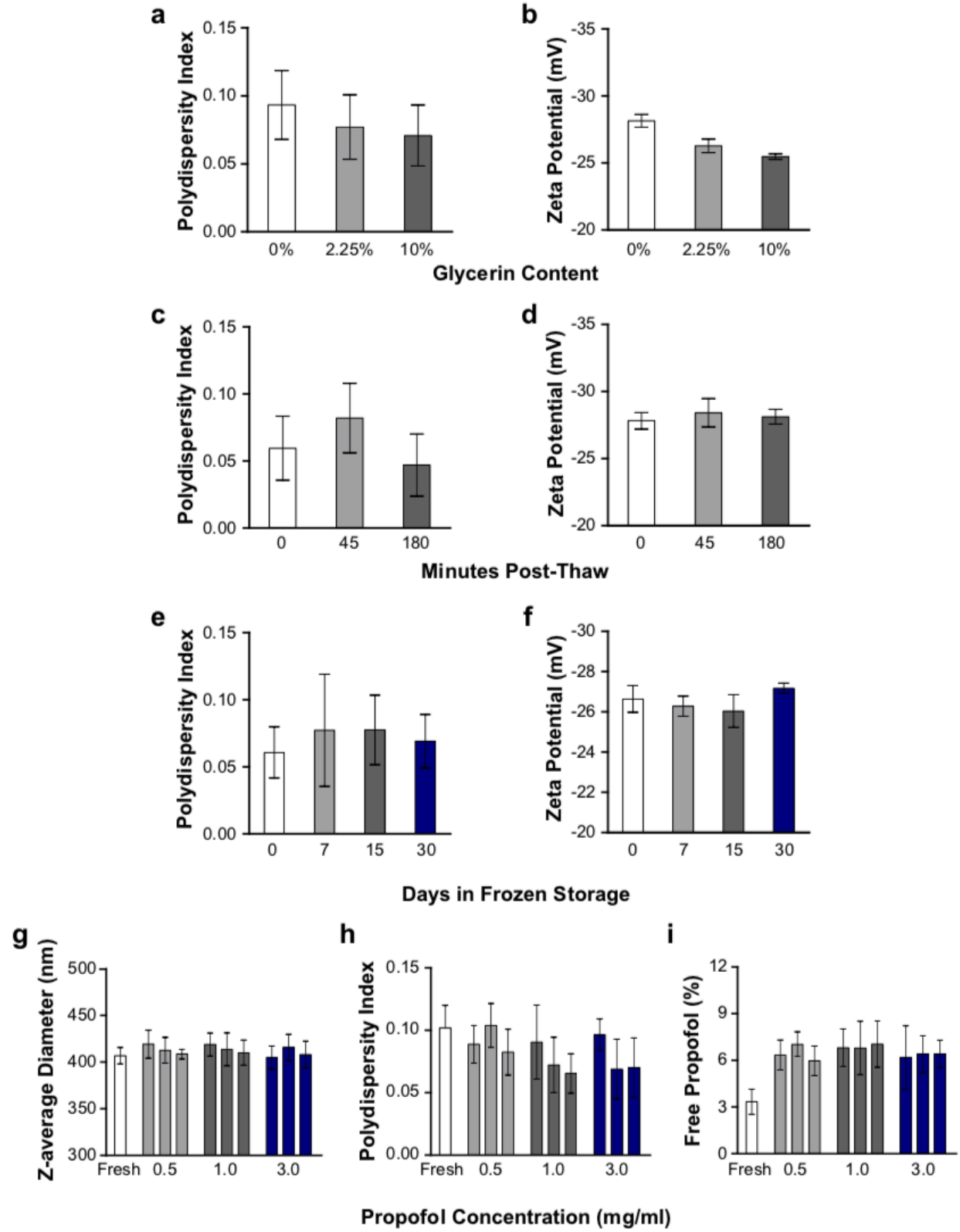
a
Polydispersity Index
0.15
0.10
0.05
0.00
0%
2.25%
10%
b
Zeta Potential (mV)
-35
-30
-25
-20
0%
2.25%
10%
Glycerin Content
c
Polydispersity Index
0.15
0.10
0.05
0.00
0
45
180
d
Zeta Potential (mV)
-35
-30
-25
-20
0
45
180
Minutes Post-Thaw
e
Polydispersity Index
0.15
0.10
0.05
0.00
0
7
15
30
f
Zeta Potential (mV)
-30
-28
-26
-24
-22
-20
0
7
15
30
Days in Frozen Storage
g
Z-average Diameter (nm)
500
450
400
350
300
Fresh
0.5
1.0
3.0
h
Polydispersity Index
0.15
0.10
0.05
0.00
Fresh
0.5
1.0
3.0
i
Free Propofol (%)
12
9
6
3
0
Fresh
0.5
1.0
3.0
Propofol Concentration (mg/ml)

Fig. S4. Stability of propofol-loaded nanoemulsions. (a) Polydispersity index and **(b)** zeta potential of propofol-loaded nanoemulsions with different contents of glycerin. **(c)** Polydispersity index and **(d)** zeta potential of propofol-loaded nanoemulsions at the indicated amount of time post thaw from frozen. **(e)** Polydispersity index and **(f)** zeta potential of propofol-loaded nanoemulsions stored frozen for 0 (fresh), 7, 15, and 30 days. **(g)** Z-average diameter, **(h)** polydispersity index and **(i)** percent of free propofol in suspensions of propofol-loaded nanoemulsions with different propofol concentrations (0.5-3 mg/ml), post thaw from frozen, compared with fresh unfrozen nanoemulsions. The glycerin content in nanoemulsions is 2.25%, w/v and 3 batches with the same concentration were measured in **(c)** – **(i)**.

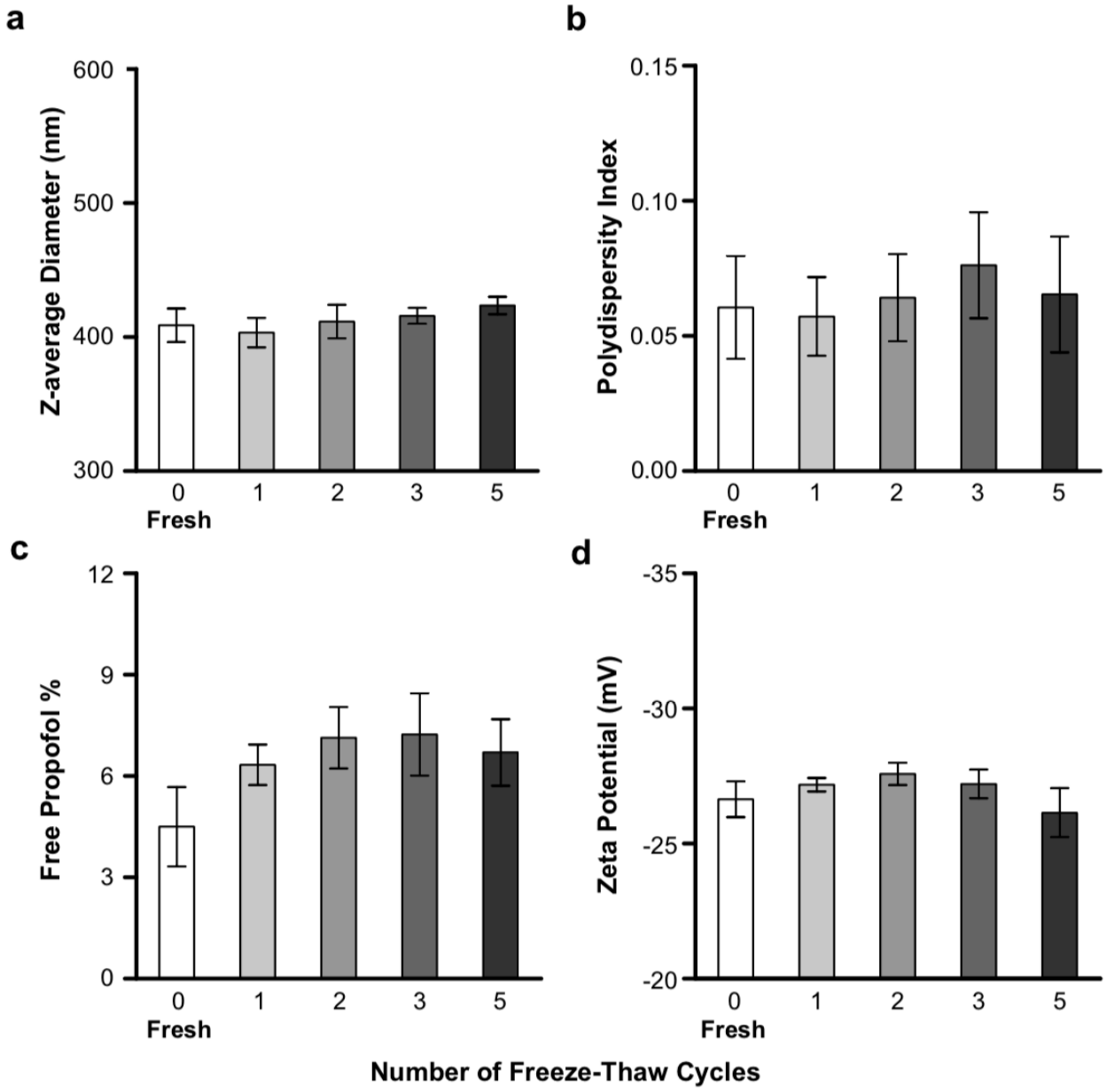

Fig. S5. **Propofol-loaded nanoemulsions are stable across multiple freeze-thaw cycles**. **(a)** Z-average diameter, **(b)** polydispersity index, **(c)** free drug fraction and **(d)** zeta potential of propofol-loaded nanoemulsions across freeze-thaw cycles.

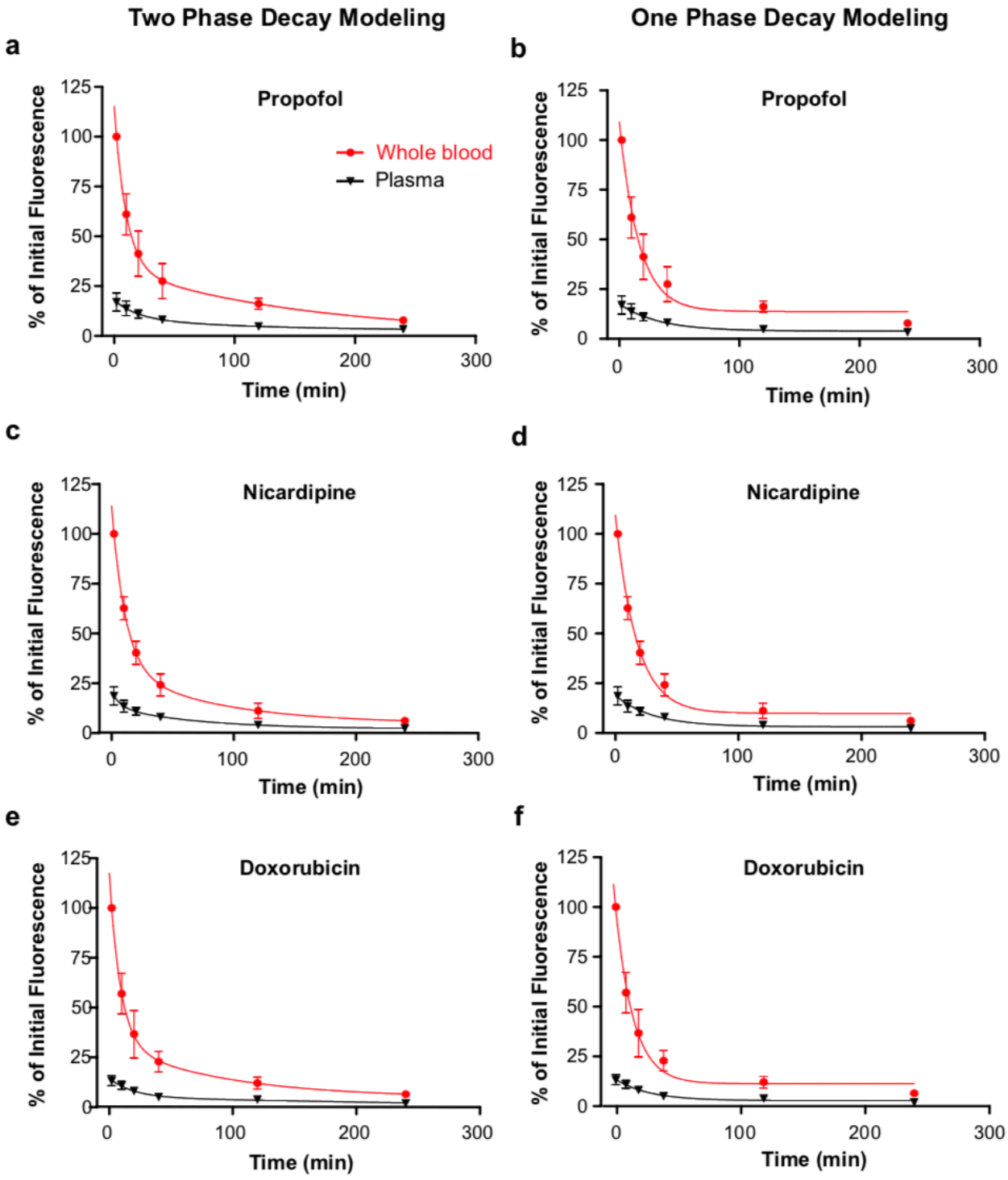

Fig. S6. **Two-phase decay and one-phase decay modeling of blood-pool kinetics of nanoemulsions after bolus administration**. **(a)**, (**b)** Propofol-loaded nanoemulsions. **(c)**, **(d)** Nicardipine-loaded nanoemulsions. **(e)**, **(f)** Doxorubicin-loaded nanoemulsions.

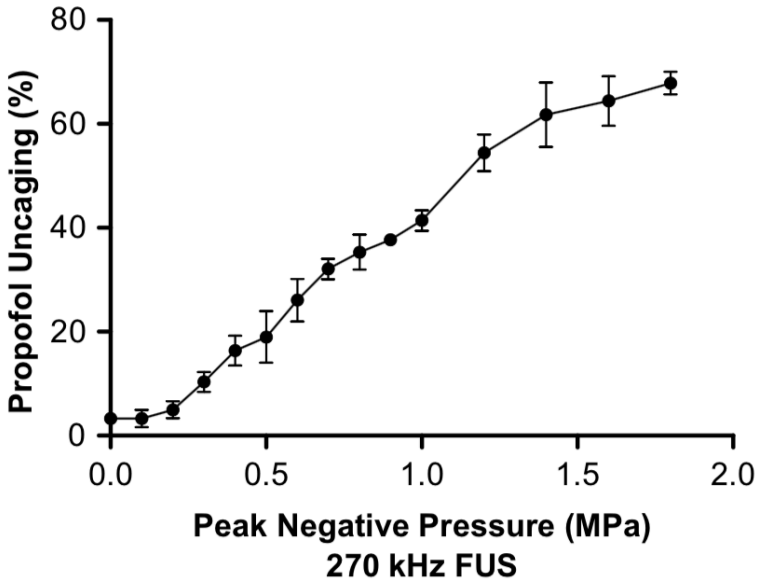

Fig. S7. **Effective ultrasonic drug uncaging *in vitro* with a 270 kHz transducer** (60 repetitions of 50 ms pulses with 950 ms pauses at 1 Hz pulse repetition frequency) for thawed nanoparticles.

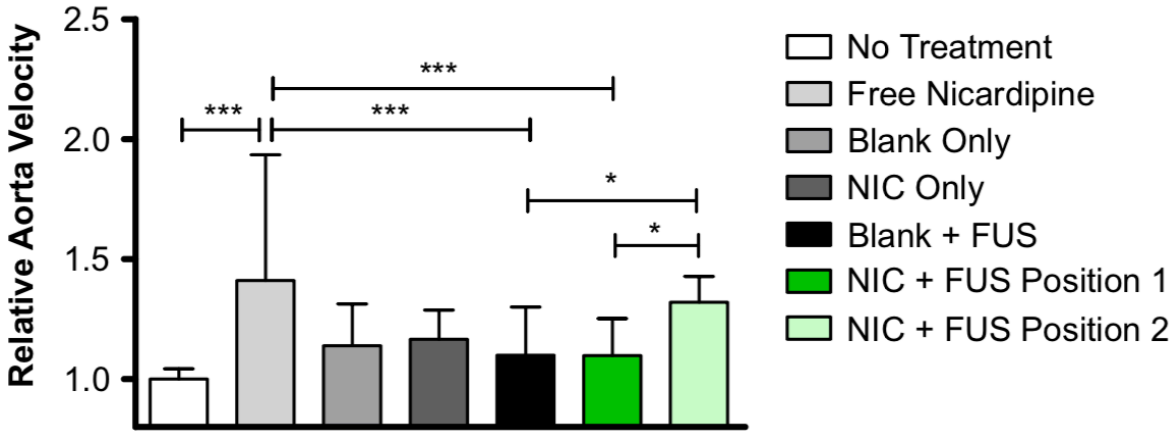

Fig. S8. **Ultrasonic nicardipine uncaging in the distal aorta selectively increases the blood flow velocity in the aorta.** Free nicardipine administration increases the average systolic velocity of the rat abdominal aorta at 14 min, normalized by the initial (0 s) values. Uncaging nicardipine-loaded nanoparticles in the distal aorta (Position 2) similarly increases the systolic velocity, although this was not seen with uncaging in the proximal aorta (Position 1). FUS: focused ultrasound application (650 kHz, 240 repetitions of 50 ms pulses with 950 ms pauses at 1 Hz pulse repetition frequency, 1.5 MPa est. peak *in situ* pressure), NIC: Nicardipine-loaded nanoparticles. Free nicardipine and NIC administered to total drug dose of 134 µg/kg i.v. Mean +/- S.D. are presented for groups of N=5-6. **: $p < 0.05$; ***: $p < 0.001$ by ANOVA ($F(6, 178) = 9.385$) with Tukey's post-hoc tests.

Table S1. **R^2 of blood-pool kinetics modeling.**

	Two-phase decay			One-phase decay		
	Propofol	Nicardipine	Doxorubicin	Propofol	Nicardipine	Doxorubicin
Whole blood	0.9639	0.9881	0.9698	0.9283	0.9608	0.9484
Plasma	0.8311	0.8850	0.9080	0.8023	0.8462	0.8801

Table S2. **Half-life of ultrasonically uncaged propofol and nicardipine *in vivo* from polymeric PFP nanoemulsions. The half-life was obtained via two-phase decay modeling.**

Plasma half life	Propofol (min)				Nicardipine (min)			
	Femoral	R^2	Jugular	R^2	Femoral	R^2	Jugular	R^2
Short phase $t_{1/2\alpha}$	1.0	0.9535	0.7	0.9703	2.1	0.9414	1.6	0.9574
Long phase $t_{1/2\beta}$	14.4		7.5		12.9		10.1	

Note: The sonication condition is 650 kHz, 240 repetitions of 50 ms pulses with 950 ms pauses s at 1 Hz pulse repetition frequency

Video S1. Ultrasound acquisition of the rat abdominal aorta prior to ultrasonic nicardipine uncaging. A 10 MHz ultrasound imaging transducer was positioned over the distal abdominal aorta (yellow arrows). The cine clip demonstrates relatively little movement of the aortic wall between the systole and diastole of the cardiac cycle. The scale bar is 1 mm.

Video S2. Ultrasound acquisition of the rat abdominal aorta following ultrasonic nicardipine uncaging. A 10 MHz ultrasound imaging transducer was positioned over the distal abdominal aorta (yellow arrows), and the sonication probe was positioned over the proximal aorta. The cine clip obtained 14 minutes post ultrasonic nicardipine uncaging demonstrates increased distensibility of the aorta, as indicated by more dynamic movement of the aortic wall during the cardiac cycle. The scale bar is 1 mm.

Supplementary References:

[1] M. Basotra, S.K. Singh, M. Gulati, Development and Validation of a Simple and Sensitive Spectrometric Method for Estimation of Cisplatin Hydrochloride in Tablet Dosage Forms: Application to Dissolution Studies, ISRN Analytical Chemistry. 2013 (n.d.) 8. doi:https://doi.org/10.1155/2013/936254.

[2] L. Xing, T.-C. Li, N. Mayazaki, M.N. Simon, J.S. Wall, M. Moore, C.-Y. Wang, N. Takeda, T. Wakita, T. Miyamura, R.H. Cheng, Structure of Hepatitis E Virion-sized Particle Reveals an RNA-dependent Viral Assembly Pathway, J. Biol. Chem. 285 (2010) 33175–33183. doi:10.1074/jbc.M110.106336.

[3] K. Xiao, Y. Li, J.S. Lee, A.M. Gonik, T. Dong, G. Fung, E. Sanchez, L. Xing, H.R. Cheng, J. Luo, K.S. Lam, "OA02" Peptide Facilitates the Precise Targeting of Paclitaxel-Loaded Micellar Nanoparticles to Ovarian Cancer In Vivo, Cancer Res. (2012). doi:10.1158/0008-5472.CAN-11-3883.